On the origin and movement of the poles in the coupled channels model for $\bar{K}N$ interactions

Aleš Cieplý

Nuclear Physics Institute, Řež/Prague, Czechia

model formulated with J. Smejkal

significant contribution by L. Hrazdilová

LEANNIS meeting, Praha, May 21, 2012

Outline

- A.C., J. Smejkal - Nucl. Phys. A 881 (2012) 115
- A.C., E. Friedman, A. Gal, D. Gazda, J. Mareš - Phys. Lett. B 702 (2011) 402, Phys. Rev. C 84 (2011) 045206
- L. Hrazdilová - graduate thesis, Czech Technical Uviversity (2012)

Introduction

$\bar{K}N$ interaction

strongly interacting multichannel system with an s-wave resonance, the $\Lambda(1405)$, just below the $K^- p$ threshold

$\downarrow\downarrow\downarrow$

$\bar{K}$-nucleus interaction

strongly attractive and absorptive, $V_{\rm opt}(\rho) \sim t_{\bar{K}N}(\rho)\, \rho$

? optical potential depth: phenomenology $V_{\rm opt}$=**(150-200)** MeV
chiral models $V_{\rm opt}$=**(50-60)** MeV

? existence of sufficiently narrow K^-–nuclear bound states

$\downarrow\downarrow\downarrow$

kaon propagation in nuclear matter

heavy ion collisions

? kaon condensation, neutron star structure

Introduction

A modern theoretical treatment of $\bar{K}N$ interaction is based on an effective chiral Lagrangian (a concept introduced by Weinberg for the πN interaction)

- ChPT implements the QCD symmetries in it's nonperturbative regime
- coupled channels techniques are used to deal with divergencies due to resonances in the strangeness $S = -1$ sector
- $\Lambda(1405)$ resonance generated dynamically; two $I = 0$ poles
- the leading order Tomozawa-Weinberg interaction does surprisingly well but NLO terms are necessary to achieve a good qualitative reproduction of the low energy $K^- p$ data
- new precise data on the 1s energy level characteristics in the kaonic hydrogen atom from SIDDHARTA experiment (plus the kaonic deuterium should follow soon)

OUR WORK: simultaneous description of the K-atomic and low energy $K^- p$ data to fix model parameters, then the model is used to study its pole content and movement of the poles on the complex energy manifold

Separable meson-baryon potentials

the model describes interactions of the lightest meson and baryon octets:

$$\phi = \begin{pmatrix} \pi^0 + \frac{1}{\sqrt{3}}\eta & \sqrt{2}\pi^+ & \sqrt{2}K^+ \\ \sqrt{2}\pi^- & -\pi^0 + \frac{1}{\sqrt{3}}\eta & \sqrt{2}K^0 \\ \sqrt{2}K^- & \sqrt{2}\bar{K}^0 & -\frac{2}{\sqrt{3}}\eta \end{pmatrix} \qquad B = \begin{pmatrix} \frac{1}{\sqrt{2}}\Sigma^0 + \frac{1}{\sqrt{6}}\Lambda & \Sigma^+ & p \\ \Sigma^- & -\frac{1}{\sqrt{2}}\Sigma^0 + \frac{1}{\sqrt{6}}\Lambda & n \\ \Xi^- & \Xi^0 & -\frac{2}{\sqrt{6}}\Lambda \end{pmatrix}$$

10 coupled $Q = 0$ channels:	$\pi^0\Lambda$	~ 1250 MeV
	$\pi^0\Sigma^0$, $\pi^-\Sigma^+$, $\pi^+\Sigma^-$	~ 1330 MeV
	K^-p, $\bar{K}^0 n$	~ 1430 MeV
	$\eta\Lambda$, $\eta\Sigma^0$	~ 1700 MeV
	$K^0\Xi^0$, $K^+\Xi^-$	~ 1800 MeV
6 coupled $Q = -1$ channels:	$\pi^-\Lambda$	~ 1250 MeV
	$\pi^-\Sigma^0$, $\pi^0\Sigma^-$	~ 1330 MeV
	K^-n	~ 1430 MeV
	$\eta\Sigma^-$	~ 1700 MeV
	$K^0\Xi^-$	~ 1800 MeV

Separable meson-baryon potentials

We employ the effective chiral model of Kaiser, Siegel and Weise (1995) with the s-wave meson-baryon Lagrangian up to the second order, the heavy baryon formulation

Parameters: f_π, f_K, f_η - meson decay constants

M_0 - baryon octet mass

$D \simeq 3/4$, $F \simeq 1/2$ - axial vector couplings, $g_A = F + D$

b_0, b_D, b_F, four d's - second order couplings

Schematic picture (taken from Borasoy, Nissler, Weise - 2005):

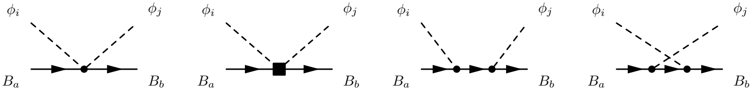

$\mathcal{O}(q^1)$ contact $\mathcal{O}(q^2)$ contact   direct s-term   crossed u-term

Separable meson-baryon potentials

Problem: χPT is not applicable in the resonance region!
Solution: effective separable potentials constructed to match the chiral amplitudes up to $\mathcal{O}(q^2)$

$$V_{ij}(k,k';\sqrt{s}) = \sqrt{\frac{1}{2\omega_i}\frac{M_i}{E_i}}\, g_i(k^2)\, \frac{C_{ij}(\sqrt{s})}{f_i\, f_j}\, g_j(k'^2)\, \sqrt{\frac{1}{2\omega_j}\frac{M_j}{E_j}}$$

Lippmann-Schwinger equation used to solve exactly the loop series

- kinematical factors guarantie a proper relativistic flux normalization with ω_i, M_i and E_i denoting the meson energy, the baryon mass and energy in the meson-baryon CMS
- coupling matrix C_{ij} determined by the chiral SU(3) symmetry, includes terms up to second order in the meson c.m. kinetic energies
- the formfactors $g_j(k) = 1/[1+(k/\alpha_j)^2]$ account naturally for the off-shell effects with the inverse ranges α_j fitted to the low energy $\bar{K}N$ data
- our approach differs from the more popular on-shell scheme based on the Bethe-Salpeter equation and the unitarity relation for the inverse of the T-matrix

Data reproduction

Threshold branching ratios:

$$
\begin{aligned}
\gamma &= \frac{\sigma(K^- p \to \pi^+\Sigma^-)}{\sigma(K^- p \to \pi^-\Sigma^+)} = 2.36 \pm 0.04 \ , \\
R_c &= \frac{\sigma(K^- p \to \text{charged particles})}{\sigma(K^- p \to \text{all})} = 0.664 \pm 0.011 \ , \\
R_n &= \frac{\sigma(K^- p \to \pi^0\Lambda)}{\sigma(K^- p \to \text{all neutral states})} = 0.189 \pm 0.015.
\end{aligned}
$$

$K^- p$ cross sections to six different meson-baryon final states:

at the $p_{LAB} = 110$ MeV for the $K^- p$, $\bar{K}^0 n$, $\pi^+\Sigma^-$, $\pi^-\Sigma^+$
at the $p_{LAB} = 200$ MeV for the above channels plus $\pi^0\Lambda$, $\pi^0\Sigma^0$

Data reproduction

Kaonic hydrogen characteristics:

strong interaction energy shift	$\Delta E_N(1s)$
the decay width	$\Gamma(1s)$

two recent measurements at at DAΦNE in Frascati:

DEAR (2005)	$\Delta E_N(1s) = 193 \pm 37(stat.) \pm 6(syst.)$ eV $\Gamma(1s) = 249 \pm 111(stat.) \pm 39(syst.)$ eV
SIDDHARTA (2011)	$\Delta E_N(1s) = 283 \pm 36(stat.) \pm 6(syst.)$ eV $\Gamma(1s) = 541 \pm 89(stat.) \pm 22(syst.)$ eV

our approach - direct numerical solution of the $K^- p$ bound state problem, no Deser-like relation to the $K^- p$ scattering length

Data reproduction

Fit to 15 experimental data:

3 branching ratios, 2 kaonic hydrogen characteristics, 10 cross sections

TW1 only the leading order (LO) Tomozawa-Weinberg interaction,
two parameters: $\alpha_i = \alpha_{TW} = 701$ MeV, $f_i = f_{TW} = 113$ MeV

NLO30 LO+NLO interactions, couplings f_i fixed at physical values
$f_\pi = 92.4$ MeV, $f_K = 110.0$ MeV and $f_\eta = 118.8$ MeV,
inverse ranges of channels closed at the $\bar{K}N$ threshold set to
$\alpha_{\eta\Lambda} = \alpha_{\eta\Sigma^0} = \alpha_{K\Xi} = 700$ MeV;
fitted 3 inverse ranges and 4 NLO d–couplings

CS30 LO+NLO model taken from our previous work, included DEAR data instead of SIDDHARTA

inverse ranges (in MeV) and d–couplings (in GeV^{-1}):

model	$\alpha_{\pi\Lambda}$	$\alpha_{\pi\Sigma}$	$\alpha_{\bar{K}N}$	d_0	d_D	d_F	d_1
CS30	291	601	639	−0.450	0.026	−0.601	0.235
NLO30	297	491	700	−0.812	0.288	−0.737	−0.016

Data reproduction

$K^- p$ threshold data calculated in several LO and LO+NLO coupled-channel chiral models.

model	ΔE_{1s}	Γ_{1s}	γ	R_c	R_n	z_1(I=0)	z_2(I=0)
TW1	323	659	2.36	0.636	0.183	(1371, −54)	(1433, −25)
JOR	275*	586*	2.30	0.618	0.257	(1389, −64)	(1427, −17)
IHW	373*	495*	2.36	0.66	0.20	(1384, −90)	(1422, −16)
NLO30	310	607	2.37	0.660	0.191	(1355, −86)	(1418, −44)
CS30	260	692	2.37	0.655	0.188	(1398, −51)	(1441, −76)
BNW	236*	580*	2.35	0.653	0.194	(1408, −37)	(1449, −106)
IHW	306*	591*	2.37	0.66	0.19	(1381, −81)	(1424, −26)
exp.	283	541	2.36	0.664	0.189	–	–
error (±)	42	111	0.04	0.011	0.015	–	–

Data reproduction

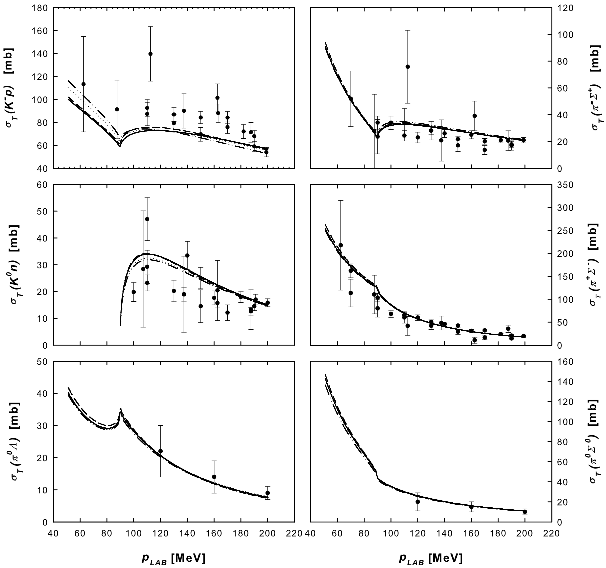

Data reproduction

$\pi\Sigma$ mass distribution: comparison with results taken from three "compatible" experiments (Thomas, Hemingway, ANKE@COSY)

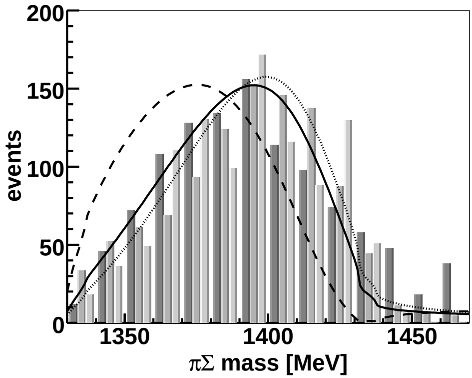

$$dN_{\pi\Sigma}/dM \sim \left| T_{\pi\Sigma,\pi\Sigma}(I=0) + r_{KN/\pi\Sigma}\ T_{\pi\Sigma,\bar{K}N}(I=0) \right|^2 p_{\pi\Sigma}$$

Free space $\bar{K}N$ amplitudes

Energy dependence of the real (left panel) and imaginary (right panel) parts of the elastic K^-p amplitude in the free space. Dashed curves: TW1 model, dot-dashed: CS30 model, solid curves: NLO30 model.

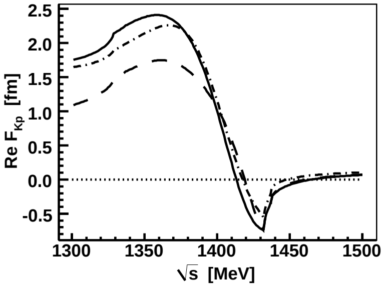

Free space $\bar{K}N$ amplitudes

Energy dependence of the real (left panel) and imaginary (right panel) parts of the elastic $K^{-}n$ amplitude in the free space. Dashed curves: TW1 model, dot-dashed: CS30 model, solid curves: NLO30 model.

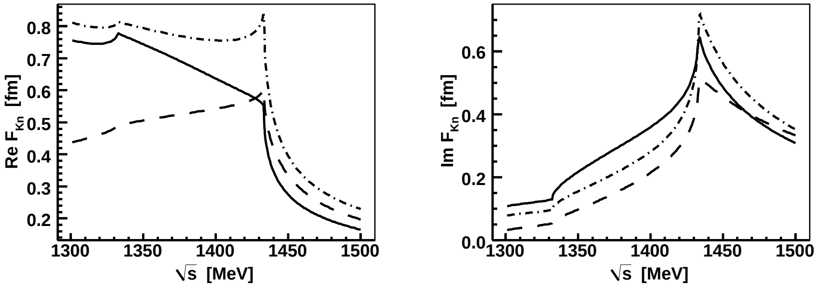

Free space $\bar{K}N$ amplitudes

Energy dependence of the real (left panel) and imaginary (right panel) parts of the isoscalar (continuous line) and isovector (dashed line) $\bar{K}N$ elastic amplitudes for the NLO30 model.

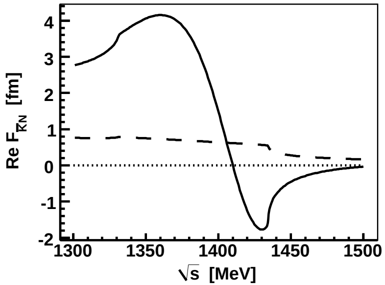

Dynamically generated resonances/poles

$\Lambda(1405)$ = two overlaping dynamical resonances? (Oller and Meissner, 2001)

- couplings of the poles to $\bar{K}N$ and $\pi\Sigma$ are different
- decay spectrum should depend on production mechanismus
- Borasoy, Nissler, Weise (2005): the formation of a pronounced double pole structure close to real axis occurs only in the TW model
- Ikeda, Hyodo, Weise (2011): the pole positions seen in their TW model can be reproduced with the LO+NLO model too
- current experimental measurements of the $\pi\Sigma$ mass spectrum in various reactions are not conclusive
  - "standard" $\pi\Sigma$ spectra compatible with a peak around 1400 MeV
  - $K^- p \longrightarrow \pi^0\pi^0\Sigma^0$ reaction (Prakhov et al., Crystall Ball Collaboration) shows a peak at 1420 MeV but the analysis of the experimental results has been put in question
  - a resonance at $\sqrt{s} \approx 1425$ MeV argued in an analysis by Jido, Oset and Sekihara (2009) for a rather old process on deuteron target, $K^- d \longrightarrow \pi\Sigma n$

Dynamically generated resonances/poles

The positions of the isoscalar poles assigned to the $\Lambda(1405)$ and $\Lambda(1670)$ resonances.
Each model generates two poles assigned to the $\Lambda(1405)$ resonance.

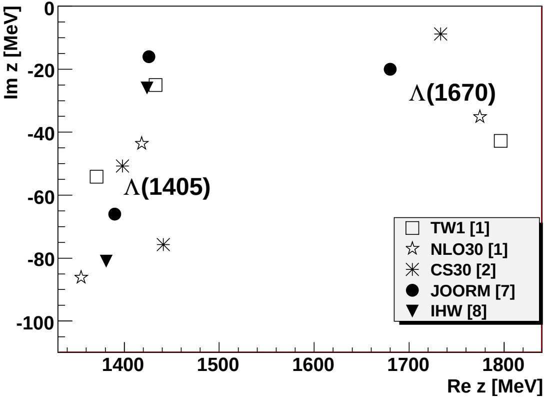

Dynamically generated resonances/poles

Where the poles come from?

The elementary amplitude can be obtained as a solution of algebraic equation for the f-matrix:

$$f_{ij}(\sqrt{s}) = \left[(1 - v \cdot G(\sqrt{s}))^{-1} \cdot v\right]_{ij} \quad , \quad v_{ij} = -\frac{C_{ij}}{4\pi f_i f_j}\sqrt{\frac{M_i M_j}{s}}$$

$$G_n(\sqrt{s}) = -4\pi \int \frac{d^3p}{(2\pi)^3} \frac{g_n^2(p^2)}{k_n^2 - p^2 + \mathrm{i}0} = \frac{(\alpha_n + \mathrm{i}k_n)^2}{2\alpha_n}\,[g_n(k_n)]^2$$

The amplitude has poles for complex energies z (equal to $\sqrt{s}$ on the real axis) if a determinant of the inverse matrix is equal to zero,

$$\det|f^{-1}| = \det|v^{-1} - G| = 0$$

When the parameters of the model are varied the poles move on the complex energy manifold and can move from one Riemann sheet to another one by crossing the real axis.

Dynamically generated resonances/poles

The origin of the poles can be traced to

the zero coupling limit: $C_{ij} = 0$ for $i \neq j$ (interchannel couplings switched off)

for $C_{i,j\neq i} = 0$ the condition for a pole of the amplitude becomes

$$\prod_n [1/v_{nn} - G_n] = 0$$

There will be a pole in channel n at a Riemann sheet $+/-$ if the following condition is satisfied for any complex energy z:

$$1/v_{nn} - G_n(z[+/-]) = 0$$

Once we have the solutions (pole positions) we can follow their movements on the complex energy manifold by gradually turning on the interchannel couplings.

Only states with nonzero diagonal couplings $C_{i,j=i}$ can generate the poles!

Dynamically generated resonances/poles

$$
C_{ij}^{I=0} = \begin{array}{c} \begin{array}{cccc} \pi\Sigma & \bar{K}N & \eta\Lambda & K\Xi \end{array} \\ \begin{pmatrix} 4 & -\sqrt{3/2} & 0 & \sqrt{3/2} \\ & 3 & 3\sqrt{1/2} & 0 \\ & & 0 & -3\sqrt{1/2} \\ & & & 3 \end{pmatrix} \end{array}
\qquad
C_{ij}^{I=1} = \begin{array}{c} \begin{array}{ccccc} \pi\Lambda & \pi\Sigma & \bar{K}N & \eta\Lambda & K\Xi \end{array} \\ \begin{pmatrix} 0 & 0 & -\sqrt{3/2} & 0 & -\sqrt{3/2} \\ & 2 & -1 & 0 & 1 \\ & & 1 & -\sqrt{3/2} & 0 \\ & & & 0 & -\sqrt{3/2} \\ & & & & 1 \end{pmatrix} \end{array}
$$

For both isospins, $I = 0$ and $I = 1$ the poles can be in the $\pi\Sigma$, $\bar{K}N$ and $K\Xi$ channels.
We have three isoscalar poles and three isovector poles. No more and no less!

Notation: Each Riemann sheet is labeled by the signs of the imaginary parts of the CMS momenta in the meson-baryon channels ordered according to their thresholds.

For $I = 0$ the RS [+,+,+,+] is the physical sheet, for $I = 1$ it is the [+,+,+,+,+] RS.
The Riemann sheets accessed by crossing the real axis in between the $\pi\Sigma$ and $\bar{K}N$ thresholds are [-,+,+,+] and [-,-,+,+,+], respectively.

Dynamically generated resonances/poles

Pole movements upon scaling the nondiagonal interchannel couplings. Left panel: isoscalar states, right panel: isovector states. The large solid and empty circles show the pole positions in the physical and zero coupling limits, respectively.

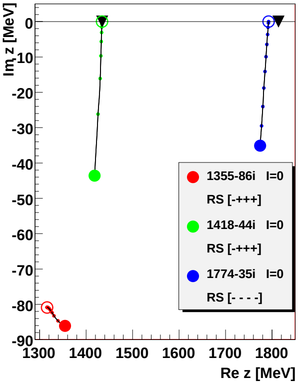

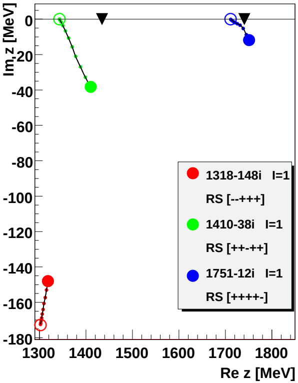

The $I = 1$ pole evolving from the $K\Xi$ channel can be assigned to $\Sigma(1750)$, a three star resonance observed in the $\pi\Lambda$, $\pi\Sigma$, $\bar{K}N$ and $\eta\Sigma$ spectra.

SU(3) restoration

Pole movements upon scaling the hadron masses to their SU(3) limits were reported in
D. Jido, J.A. Oller, E. Oset, A. Ramos and U.-G. Meissner, *Nucl. Phys.* **A 725** (2003) 181

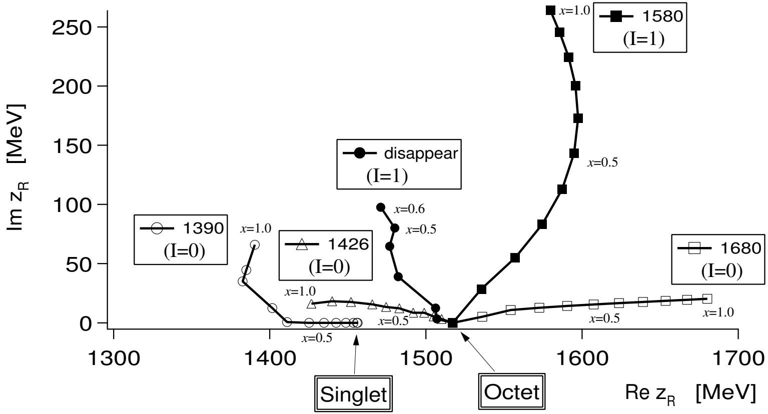

SU(3) restoration

The picture differs in some respects from what we get with our TW1 model:

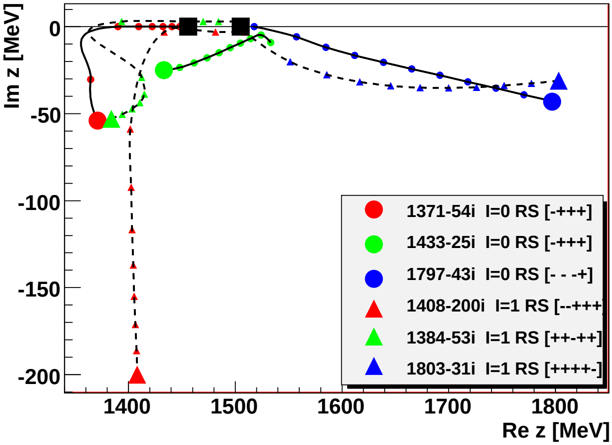

SU(3) restoration

How it is done:

$$M_i(x_{SU3}) = M_0 + x_{SU3}(M_i - M_0) \quad , \quad m_i^2(x_{SU3}) = m_0^2 + x_{SU3}(m_i^2 - m_0^2)$$

The hadron masses in the $SU(3)$ chiral limits represented by $m_0 = 370$ MeV for the mesons and $M_0 = 1150$ MeV for the baryons.

The situation around $x_{SU3} \approx 0.6$:

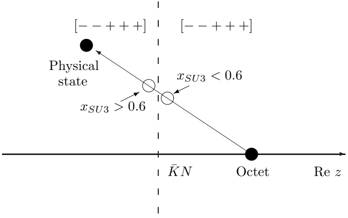

The thresholds move upon scaling the masses! So do the poles.
Jido et. al. searched the poles on a "combined" Rieman sheet with discontinuities along lines perpendicular to the real axis at the threshold energies. They searched for the pole on the [-,-,-,+,+] RS above the $\bar{K}N$ threshold and on the [-,-,+,+,+] RS below the threshold.

Summary

- The chirally motivated model for $\bar{K}N$ interactions generates three $I = 0$ poles (assigned to $\Lambda(1405)$ and $\Lambda(1670)$) and three $I = 1$ poles (a structure in the $K^- n$ amplitude, $\Sigma(1750)$, one of them too far from the physical region).
- The pole positions are model dependent, though the models restricted to the TW coupling tend to agree on the position of the $I = 0$ pole related to the $\bar{K}N$ channel.
- Pole movements on the complex energy manifold give us additional insights on the origin of the dynamically generated meson-baryon resonances.
- The model was successfully used in in-medium applications (kaonic atoms, kaon nuclear quasi–bound states, hypernuclear production) not covered in this talk.